

**TARGETED REPLACEMENT OF MOUSE APOLIPOPROTEIN A-I WITH HUMAN  
APOA-I OR THE MUTANT APOA-IMilano:  
EVIDENCE OF APOA-IM IMPAIRED HEPATIC SECRETION\***

**Cinzia Parolini<sup>‡,°</sup>, Giulia Chiesa<sup>‡</sup>, Yiwen Zhu<sup>§</sup>, Trudy Forte<sup>§</sup>, Silvia Caligari<sup>‡</sup>,  
Elisabetta Gianazza<sup>‡</sup>, Maria Grazia Sacco<sup>¶</sup>, Cesare R. Sirtori<sup>‡</sup>, and Edward M.  
Rubin<sup>§</sup>**

*From the <sup>‡</sup>Department of Pharmacological Sciences, University of Milan, 20133  
Milan, Italy, <sup>¶</sup>ITB-CNR, 20090 Segrate (Milan), Italy, <sup>§</sup>Genome Sciences  
Department, Lawrence Berkeley National Laboratory, Berkeley, California 94720,  
USA*

\* The research was conducted at the E.O. Lawrence Berkeley National Laboratory and at Department of Pharmacological Sciences, Milano. This work was supported in part by a grant from the National Institute of Health, National Heart, Lung, and Blood Institute, HL18574 and National Institute of Health, National Heart, Lung and Blood Institute, HL55493, and Department of Energy Contract DE-AC0376SF00098, University of California, Berkeley, California, USA. Moreover, this work was in part supported by Ministero dell'Università e della Ricerca Scientifica e Tecnologica of Italy (grant 9806174392), by Istituto Superiore di Sanità (grant 96/H/T15 and 93-99/H/T12), and by a grant from Esperion Therapeutics, Ann Arbor, MI, USA. In addition, the financial support of FIRB/MIUR to P. V. and of AIRC to M.G. S. is

gratefully acknowledged. This is manuscript No. 65 of the Genoma 2000 Project funded by CARIPLO.

**°To whom correspondence should be addressed: Department of Pharmacological Sciences, University of Milan, via Balzaretti 9, 20133 Milan, Italy. Tel.: 39+02+50318328; Fax: 39+02+50318284; E-mail: cinzia.parolini@unimi.it**

**Running title: Impaired apoA-IM secretion in a knock-in mouse model**

**1 The abbreviation used are: HDL, high density lipoproteins; C, cholesterol; apo, apolipoprotein; A-IM, A-IMilano; k-in, knock-in; Kb, Kilobase; bp, base pairs; PCR, polymerase chain reaction; ES, embryonic stem cell; TG, triglycerides; GGE, gradient gel electrophoresis; 2-DE, two-dimensional electrophoresis;  $\beta$  ME,  $\beta$  mercaptoethanol; SDS-PAGE, SDS-polyacrylamide gel electrophoresis.**

## SUMMARY

Despite a pro-atherogenic profile, individuals carrying the molecular variant (R173C) of apolipoprotein (apo)A-I, named apoA-IMilano (apoA-IM), appear to be at reduced risk for cardiovascular disease. To develop an *in vivo* system to explore, in a controlled manner, the effects of apoA-IM on lipid metabolism, we have used the gene targeting technology, or gene k-in", to replace the murine apoA-I gene with either human apoA-I or apoA-IM genes in embryonic stem cells. As in human carriers, mice expressing apoA-IM (A-IM k-in) are characterized by low concentrations of the human apolipoprotein and reduced high density lipoprotein-cholesterol (HDL-C) levels, compared to A-I k-in animals. The aim of the present study was to investigate the basic mechanisms of hypoalphalipoproteinemia associated with the apoA-IM mutation. ApoA-I and apoA-IM mRNA expression, as assessed by Northern blot analysis and quantitative real-time RT-PCR, did not exhibit significant differences in either liver or intestine. Moreover, human apolipoprotein synthesis rates were similar in the k-in lines. When the secretion rate of the human apolipoproteins was assessed in cultured hepatocytes from the mouse lines, secretion from apoA-IM expressing cells was markedly reduced (42% for A-IM k-in and 36% for A-I/A-IM k-in mice) as compared to that of A-I k-in hepatocytes. These results provide the first evidence that the hypoalphalipoproteinemia in apoA-IM human carriers may be partially explained by impaired apoA-IM secretion.

## INTRODUCTION

Coronary artery disease is the most common cause of death in developed countries (1) and high density lipoprotein-cholesterol (HDL-C) concentrations are a major predictor of risk. Indeed, nearly half of all patients with coronary artery disease have low HDL-C (2, 3). Low HDL-C appears to be associated with, among other factors, an enhanced risk of angioplasty restenosis (4) and with a number of clinical syndromes such as the “metabolic syndrome”, that combines low HDL with hypertriglyceridemia and abdominal obesity (5). Raising HDL-C concentrations may have therapeutic value in reducing risk of re-infarction and stroke in coronary patients (6, 7). In agreement with these clinical data, experimental studies indicate that HDL infusions are able to reduce significantly aortic lipid deposition in established atherosclerotic lesions (8-10). The cardio-protective role of HDL is, in part, related to its ability to stimulate cholesterol efflux from cells (11, 12) and by its anti-inflammatory (13) and anti-oxidant properties (14).

Genetic factors play a key role in regulating HDL-C concentrations. Changes in a variety of genes including apolipoprotein A-I/CIII (15), lipoprotein lipase (16), cholesteryl ester transfer protein (17), hepatic lipase (18), scavenger receptor B1 (19), lecithin-cholesterol acyltransferase (20), ATP-binding cassette (ABC-A1) transporter gene (21) and others, all affect to a variable extent HDL-C concentrations in humans. Several naturally occurring mutations associated with reduced plasma HDL-C and apoA-I concentrations have also been described for human apolipoprotein (apo)A-I (22, 23), the major protein constituent of HDL. Although some of these hypoalphalipoproteinemic states are associated with an

increased risk of atherosclerotic vascular disease, others do not seem to predispose to accelerated premature disease (24). One example is the apoA-IMilano (A-IM) mutant: evaluation of the cardiovascular status in apoA-IM carriers, compared to control subjects from the same kindred, did not reveal any evidence of increased vascular disease at the preclinical level (25, 26).

ApoA-IM is the result of a point mutation, with an arginine to cysteine substitution at position 173 (27). The carriers of this mutation are all heterozygotes who exhibit hypertriglyceridemia with markedly reduced HDL and apoA-I levels. The presence of a cysteine residue results in the formation of homodimers and heterodimers with apoA-II.

The kinetic etiology of hypoalphalipoproteinemias associated with apoA-I mutations have been generally related to accelerated catabolism rather than to lower synthesis of apoA-I (28, 29). However, a recent study has shown a reduced secretion rate for the apoA-I variant known as apoA-IFIN, besides its enhanced clearance from plasma (30). ApoA-I turnover in apoA-IM carriers was investigated in two different studies (31, 32). Both studies showed that low apoA-I levels are consequent to the rapid catabolism of apoA-I and apoA-IM, whereas results on the production rate of both the normal and mutant forms of apoA-I have remained controversial.

While mice expressing an A-IM transgene were previously generated and studied (33, 34), the technical limitations of microinjection (unpredictability of chromosomal location and copy number of the transgene) did not allow one to definitively establish the molecular mechanisms of the phenotypic expression of the mutation. In the present study, a gene targeting replacement strategy (gene knock-

in or k-in) was used, in order to obtain comparable mouse lines expressing either human apoA-I (A-I k-in), or human apoA-IM (A-IM k-in). Using these mouse models we present evidence that the dominant negative effects on HDL-C concentrations resulting from the apoA-IM mutation can, in part, be explained by reduced apoA-IM production. The expression of this mutation does not appear to affect transcription or mRNA stability, but causes impaired hepatic secretion of the human apolipoprotein by primary hepatocytes.

## EXPERIMENTAL PROCEDURES

*Gene Targeting Replacement*—A 3-Kb NotI-KpnI strain 129 mouse genomic fragment, containing sequences upstream of the mouse apoA-I gene (2,633 bp), and including exon 1 and the 5' part of intron 1 (104 bp) (Fig.1B), was generated by polymerase chain reaction (PCR) using a pV-90 plasmid, kindly provided by Dr. N. Maeda (35), as a template. A 4.8-Kb EcoRI strain 129 mouse genomic fragment, containing the 3'-half of exon 4 (419 bp) and 3'- flanking sequences (4,381 bp) of the mouse apoA-I gene, was also derived from pV-90 (Fig.1B). Human genomic fragments, containing the 3' part of intron 1 (116 bp), and exons 2-4 of the human apoA-I gene, or the human apoA-IM gene, were isolated by sequential digestion with KpnI and Sall from pApoA-Ig (36) and pBSM plasmids (34), respectively. To obtain the targeting constructs, the 3-Kb mouse genomic fragment and the human genomic fragments were inserted into a pPN2T vector (37) upstream of the neomycin (neo) resistant gene, whereas the 4.8-Kb genomic fragment was inserted downstream of the neo-resistant gene (Fig. 1B). The targeting constructs were

linearized by NotI digestion, purified, and redissolved in TE pH=7.4 for electroporation. A subclone of mouse strain 129 embryonic stem (ES) cell line, ESVJ (Go Germline, GenomeSystems, Inc), was cultured on neo-resistant mouse fibroblast feeder layers, electroporated with 20 µg of the linearized human apoA-I or apoA-IM targeting vectors as described previously (38). Stable integrants were selected by positive-negative selection, using neomycin (G418-Geneticin, Gibco, USA) at a final concentration of 200 µg/ml, and gancyclovir (FIAU, Moravsek Biochemicals, CA, USA) at a final concentration of 2 µM. After 10-12 days, colonies were transferred into 96-well plates, and tested for successful targeting by Southern Blotting using conventional procedures. Approximately 10 to 15 ES targeted cells were injected into the blastocoe cavity of C57BL/6J embryos. Surviving blastocysts were transferred into the pseudopregnant CD-1 females. Animals chimeric by coat color were bred to C57BL/6J animals to determine their germ-line competency. Heterozygous mutants were identified by Southern Blotting of DNA isolated from the tail, and brother-sister mating was carried out to generate homozygous k-in mutant mouse lines, expressing human apoA-I (A-I k-in) or human apoA-IM (A-IM k-in). Homozygous A-I k-in and A-IM k-in mice were then crossed to create the heterozygous human apoA-I/A-IM mouse line (A-I/A-IM k-in).

*Lipid/Lipoprotein Analyses*—Lipid and apolipoprotein analyses were performed on A-I k-in, A-IM k-in, A-I/A-IM k-in, and C57BL/6J/129 control mice of both sexes, aged 12-16 weeks. Blood was collected after an overnight fast from the retro-orbital plexus into tubes containing 0.1% (w/v) EDTA and centrifuged in a microfuge for 10 min at 8000 rpm at 4°C. Serum total and unesterified cholesterol

were measured by enzymatic methods (Hoffmann La Roche, Basel; Switzerland; Boehringer Mannheim, Mannheim, Germany) (39). Triglyceride (TG) concentrations were corrected for the free glycerol present in serum as described (Sigma-Aldrich, Germany) (40). HDL-cholesterol levels were measured after precipitation of apoB-containing lipoproteins with PEG 8000 (20% w/v) in 0.2 M glycine (pH 10) (40). Human apolipoprotein concentrations were determined by immunoturbidimetric assays, using a sheep antiserum specific for human apoA-I (Hoffmann La Roche, Basel; Switzerland) which also recognizes apoA-IM (34).

To determine HDL particle size distribution, total lipoproteins ( $d < 1.215$  g/ml) were isolated by salt gradient ultracentrifugation (41). Plasma from five fasting mice of each genotype was pooled and adjusted to a density of 1.215 g/ml with solid KBr and centrifugated for 6 hours at 4°C at 100,000 rpm in a Beckman TL100 ultracentrifuge equipped with a Beckman TL100.3 rotor. HDL particle size distribution was determined by nondenaturing polyacrylamide gradient gel electrophoresis (GGE) essentially as described by Nichols et al (42). Aliquots (20  $\mu$ l) of the total lipoprotein fraction were loaded onto a non-denaturing 4% to 30% polyacrylamide gradient gel and electrophoresed for 25 hours at 125 V at 4°C. Proteins were stained with Coomassie R-250, and HDL particle size was determined by densitometry, as previously described (42).

Two-dimensional electrophoretic (2-DE) maps of mouse sera were obtained by IPG-DALT (43). Serum was prepared by low speed centrifugation of blood collected from six fasting mice for each line. Sample load was 15  $\mu$ L serum diluted to 50  $\mu$ L with either dd water, for non-reducing conditions, or with 2%  $\beta$  mercaptoethanol ( $\beta$  ME), for reducing conditions. Proteins were first resolved



according to charge on a non-linear pH 4-10 IPG (44) in the presence of 8 M urea and 0.5% carrier ampholytes. The focused proteins were then fractionated according to size by SDS-polyacrylamide gel electrophoresis (SDS-PAGE) on 7.5-17.5% polyacrylamide gradients in the discontinuous buffer system of Laemmli (45). Interfacing between the first and second dimension occurred after equilibration with 2% SDS, for non-reducing conditions, or after protein carboxymethylation, in the presence of 2% SDS (46), for reducing conditions. Anode to cathode distance was 11 cm in the IPG gel; the anodal 8 cm were mounted head to tail on 16 x 14 cm<sup>2</sup> SDS-PAGE slabs. Proteins were stained with Coomassie R-250.

*Northern Blot Analysis*—Total RNA was extracted from mouse liver according to the method of Chomczynski and Sacchi (47), using UltraPure<sup>TM</sup> Trizol Reagent (Gibco, BRL, Life Technologies). For Northern blot analysis, 15 µg of denatured RNA was separated by formaldehyde-agarose gel electrophoresis, transferred to nylon membrane and hybridized with a human apoA-I probe that spans the majority of human exon 4; β-actin mRNA (Ambion) was used as an internal standard for normalizing total RNA loads.

*Quantitative real-time RT-PCR*—Total RNA was extracted from liver and intestine of 6 mice from each transgenic line using UltraPure<sup>TM</sup> Trizol Reagent (Gibco, BRL, Life Technologies). About 2 µg of total RNA from each sample was treated with Promega RQ1 RNase-free DNase. About 0.5 µg of DNase-treated total RNA was reverse-transcribed using TaqMan Reverse Transcription Reagents from

Applied Biosystems. PCR was performed using SYBR Green PCR Master Mix (Applied Biosystems) on an ABI Prism 7700 Sequence Detector. The selected primers used for amplification of human apoA-I cDNA were AGCTTGCTGAAGGTGGAGGT (in exon 4) and ATCGAGTGAAGGACCTGGC (in exon 3). The primers amplify a 154 bp product. 18S Internal Standard Control was from Ambion (315 bp product). A ratio of 1:1.5 of 18S primer pair:18S Competimers was used. All procedures and calculation of the results were carried out according to manufacture's recommendation.

*Hepatic human apoA-I or apoA-IM synthesis and secretion rates—*

Apolipoprotein synthesis rate was determined in primary hepatocytes isolated from A-IM k-in, A-I/A-IM k-in, and A-I k-in mice. Animals were fasted for 5 hours, anesthetized with 5% sodium pentobarbital, and hepatocytes prepared with slight modifications of a method described previously (48). Cell viability was assessed by trypan blue staining and 500,000 live cells were plated on 35-mm plates. The culture medium (Williams' medium, Sigma) was changed after 4h incubation at 37°C. The next day, to assess the human apolipoprotein synthesis rates, cells were washed once with PBS, pre-incubated for 1 h in leucine-free DMEM without serum, and then incubated for different time points up to 10 min, with 1 ml of the same medium containing 200  $\mu$ Ci/ml [ $^3$ H]-leucine (NEN, Life Sciences Products, Inc. Boston, USA). After incubation, the cells were washed three times with ice-cold PBS and subsequently lysed in cold lysis buffer containing protease inhibitors (PBS, 1% Triton X-100, 0.01% PMSF, and 0.005% aprotinin). As a control, the incorporation of radioactivity into total protein was determined after trichloroacetic acid precipitation

of cell lysates and was found to be similar among the k-in lines (data not shown). Radiolabelled human apolipoproteins were quantitatively isolated from cell lysates by immunoprecipitation using a rabbit polyclonal anti-human apoA-I antibody (DAKO, Glostrup, Denmark) that recognizes both human apoA-I and apoA-IM. The immunoprecipitate was further purified by SDS-PAGE under reducing conditions. A band corresponding to human apoA-I was excised from the gel; label was extracted with Solvable (Packard Instruments Co., Inc. Meriden, USA) and counted (49). Results were normalized to cellular protein content of each plate determined by the method of Bradford (50). The data presented are the mean of triplicate measurements and are representative of three independent experiments.

To determine apoA-I secretion rate, cells were isolated, plated and incubated essentially as described above except that conditioned medium was collected after 30, 60, 90 and 120 min. The medium was centrifuged at 12,000 x g at 4°C for 5 min to remove cell debris. Human apolipoproteins were quantitatively isolated from the medium by immunoprecipitation and then purified by SDS-PAGE under reducing conditions. A band corresponding to human apoA-I was excised from the gel and counted (49). Results were normalized to cellular protein content of each plate determined by the method of Bradford (50). The data presented are the mean of triplicate measurements and are representative of three independent experiments.

*Statistical analysis*—Differences among groups were evaluated using a one-way ANOVA followed by a Bonferroni's post-hoc test. Differences in the synthesis and secretion rate of human apolipoproteins were evaluated by linear regression.

## RESULTS

*Replacement of the mouse apoA-I gene with the human apoA-I or apoA-IM gene*—The targeting strategy used to replace the mouse apoA-I coding exons 2-4 with the human counterpart is illustrated in Fig. 1. Homologous recombination between the endogenous mouse apoA-I locus (Fig. 1A) and the targeting construct (Fig. 1B) results in a chimeric gene (Fig. 1C) where all the mouse coding sequences have been replaced with sequences coding for human apoA-I or apoA-IM. This chimeric locus retains all normal mouse regulatory elements in addition to the non-coding mouse exon 1.

Embryonic stem cell DNA, digested with HindIII and hybridized with Probe 1 (Fig. 1) revealed a 12-Kb endogenous band and a 9.1-Kb targeted band, resulting from the novel restriction site, demonstrating the correct location of the targeted gene in the 3' region (Fig. 2A). Similarly, hybridization with Probe 2 (Fig. 1) confirmed correct modification of the 5' region (data not shown). The modified locus (apoA-I or apoA-IM) was transmitted to the F1 generation from chimeras that were made from one of the targeted cell lines. Genotypes of F2 animals were determined using Southern blotting analysis of tail DNA digested with HindIII and hybridized with Probe 2, revealing a 12-Kb endogenous band and a 3.8-Kb targeted band (Fig. 2B).

*Serum distribution of human apolipoproteins*—The expression of human apoA-I or apoA-IM was assessed by 2-DE analysis on mouse serum (Fig. 3). A 28 kDa

spot was observed in each serum analyzed, corresponding either to murine apoA-I (only in control serum), human apoA-I or the monomeric form of apoA-IM. From their sequence, the pI of murine apoA-I is computed at 5.42, the pI of human apoA-I at 5.27 and the pI of human apoA-IM at 5.19, as indicated in the Fig. 3. The spots marked as “-1” superscript correspond to a post-translationally modified form that differs from the “0” superscript form for a N → D deamidation event (51). Since the charge difference at pH = pI is 1 unit both between apoA-I and apoA-IM, and between A-I0 and A-I-1, A-IM0 and A-I-1 do overlap (see in Fig. 3 the spot indicated as “A-I-1+A-IM0”). As expected, in A-IM k-in and A-I/A-IM k-in serum, an additional spot (see circle in Fig. 3, upper panel), corresponding to the dimeric form of apoA-IM (56 kDa), is visible and disappears upon sample reduction (Fig. 3, lower panel).

*Lipid and apolipoprotein concentrations*—Mouse plasma lipid and apolipoprotein concentrations are shown in Table I. The apoA-IM concentrations in A-IM k-in mice was approximately 50% of apoA-I in A-I k-in mice; the concentration of the human apolipoproteins in the apoA-I/A-IM k-in mice was the same as in A-IM k-in. Total cholesterol in A-IM k-in mice was significantly lower than that measured in every other group. The heterozygotes (A-I/A-IM k-in) had total cholesterol values intermediate to A-IM and A-I k-in mice. Plasma HDL cholesterol concentrations in A-IM k-in mice were substantially lower than those observed in A-I k-in and A-I/A-IM k-in mice (- 63% and - 50%, respectively). In addition, a significant increase in plasma unesterified to esterified cholesterol ratio was observed in A-IM k-in compared to A-I k-in mice ( $0.69 \pm 0.13$  vs  $0.41 \pm 0.02$ ,

$p < 0.001$ ), suggesting impaired cholesterol esterification in the former. In contrast to changes in cholesterol concentrations, plasma triglyceride levels were similar in all the mouse lines analyzed.

HDL particle size distribution of k-in mice was investigated by nondenaturing GGE. As seen in Fig. 4, HDL from A-I k-in mice has a homogeneous population of large particles (10.79 nm). Control mice had a similar HDL size distribution (data not shown). The GGE profile of A-IM k-in mice is heterogeneous, exhibiting a major HDL subpopulation of smaller particles (8.96 nm) and minor populations at 9.81 and 10.79 nm. In contrast, the GGE profile of A-I/A-IM k-in mice is characterized by a bimodal size distribution with a major population at 10.79 nm, and a minor one at 8.96 nm.

*Human apolipoproteins expression*—Apolipoprotein A-I or A-IM gene expression was assessed by Northern blot analysis on livers of six mice, matched for age and sex, from each one of the three lines (A-IM k-in, A-I/A-IM k-in, and A-I k-in). Data were normalized to the constitutively expressed  $\beta$ -actin, and average values are shown in Fig. 5. No significant differences were observed between human apoA-I and apoA-IM mRNA levels in the three k-in lines. This lack of difference in the human apolipoprotein expression was confirmed by quantitative real-time RT-PCR. In fact, the apoA-I/A-IM mRNA expression (normalized to the endogenous control 18S) was  $0.633 \pm 0.159$  for A-I k-in mice and  $0.593 \pm 0.244$  for A-IM k-in mice ( $p = 0.778$ ).

Quantitative real-time RT-PCR was also performed on total RNA extracted from mouse intestine; in each mouse line, intestinal expression of the human

apolipoproteins contributed for 28-32% of the total amount expressed. Similarly to what observed in livers, no differences were detected among the lines ( $p>0.05$ ).

*Analysis of human apoA-I or apoA-IM production*—Synthesis and secretion rates of the human apolipoproteins were assessed in cultured primary hepatocytes isolated from A-IM k-in, A-I/A-IM k-in, and A-I k-in mice. For the evaluation of synthesis rate, appearance of intracellular radiolabelled human apolipoproteins was measured at different time points and was found to be linear along the experimental period. The synthesis rates, calculated as the slope of the regression lines, were not different among the k-in lines (2.92 cpm/ $\mu$ g/min for A-IM k-in, 2.78 cpm/ $\mu$ g/min for A-I/A-IM k-in, and 2.89 cpm/ $\mu$ g/min for A-I k-in mice). For the secretion rate, radiolabeled apoA-I or apoA-IM was quantified in culture medium at 30, 60, 90, and 120 minutes after the addition of [ $^3$ H]-leucine. As shown in Fig. 6, secretion of apoA-I/A-IM was linear for all the k-in mouse lines ( $r= 0.906$  for A-I k-in mice,  $r= 0.934$  for A-I/A-IM k-in mice, and  $r= 0.964$  for A-IM k-in mice  $p<0.01$ ). Secretion rates, however, differed dramatically between A-I k-in mice and the other mouse lines, where secretion by apoA-IM, and apoA-I/A-IM cells was 58% and 64% ( $p<0.05$ ), respectively, of that calculated for apoA-I hepatocytes.

## DISCUSSION

In contrast to classical transgenic approaches, gene targeting replacement strategies (52) for manipulating the mouse genome allow precise location of the transgene, thus permitting direct comparisons between different genes at the same

chromosomal location. This procedure has allowed, for the first time, the generation of two animal models that differ only in the biochemical nature of the apoA-I, i.e. carrying in one case the human wild type apoA-I gene (A-I k-in) and, in the other, the apoA-IM gene (A-IM k-in). These mice provide a means to study the molecular mechanisms responsible for the lipoprotein abnormalities noted in apoA-IM human carriers.

The lipid/lipoprotein profile of A-IM k-in and A-I/A-IM k-in mice is, in many respects, similar to that of human carriers, i.e., characterized by low plasma total and HDL-C levels, compared to A-I k-in mice. Reduction in HDL-C concentrations are also associated with the appearance of a heterogeneous population of HDL particles, not present in control and A-I k-in mice. Nevertheless, most noteworthy are the differences observed between A-IM k-in and A-I/A-IM k-in mouse lines. We found that the expression of apoA-I in the A-IM k-in mouse background did not increase the plasma apolipoprotein concentrations, but did increase plasma total and HDL-C levels, and altered HDL size distribution. This difference could be explained by the fact that the absence of apoA-I, better cofactor for LCAT activity (53, 54), may impair cholesterol esterification in A-IM k-in mice, as suggested by the unesterified/esterified cholesterol ratio measured in this mouse line ( $0.69 \pm 0.13$  vs  $0.33 \pm 0.04$  in A-I/A-IM k-in mice), allowing the formation of cholesterol-poor HDL particles (34). In addition, the decreased formation of cholesteryl esters may result in a diminished core of HDL particles and hence in a reduced HDL particle size.

Differently from the apoA-IM clinical condition (55) and the transgenic model previously generated, expressing both human apoA-IM and apoA-II (33, 34), a clear rise of triglycerides in the A-IM k-in model was not observed. In the A-IM k-in line,



triglyceride elevation was, in fact, of minimal degree, and did not attain statistical significance. Moreover, A-IM k-in mice displayed an HDL size distribution which lacks a sub-population of very small particles, present in both human carriers (55) and in the previously generated A-IM/A-II transgenic mice (33, 34). A possible explanation for these differences may reside in the absence of human apoA-II in A-IM k-in mice. Overexpression of human apoA-II has been shown, in fact, to be associated with hypertriglyceridemia and small HDL particles (56). Moreover, in human carriers and in A-IM/A-II transgenic mice the presence of human apoA-II allows the formation of A-IM/A-II heterodimers, since the human apoA-II contains a free cysteine residue, not present in the murine apoA-II. Franceschini et al. (55) found a correlation between hypertriglyceridemia and abundance of small HDL particles (HDL<sub>3b</sub>), enriched in A-IM/A-II heterodimers. Furthermore, experimental data have shown that the expression of human apoA-II in apoA-I transgenic mice increased plasma triglyceride levels, and restricted HDL particle size (40). In summary, although speculative, in the absence of human apoA-II, i.e., in the present k-in mouse model, triglyceride metabolism is not affected by the presence of the apoA-I mutant, thus accounting for normal triglyceride levels in A-IM k-in and A-I/A-IM k-in mice.

A major objective of the present study was to utilize the k-in mice to explore the possibility that hypoalphalipoproteinemia associated with apoA-IM is due to defective expression of the human apoA-IM gene. Quantitative real-time RT-PCR on liver mRNA, coherent with Northern blot analysis, did not show any significant difference in the apoA-I and apoA-IM gene expression, revealing that neither

transcription nor mRNA stability is responsible for the low apoA-IM plasma levels. Moreover, since the intestine contributes significantly to the apoA-I expression, we have also performed quantitative real-time RT-PCR on mouse intestine and, having obtained similar results among the mouse lines, we could demonstrate that differences between the plasma levels of apoA-I and A-IM are not a consequence of a lower intestinal apoA-IM mRNA expression. Differences in apolipoprotein plasma levels cannot also be attributed to an altered apoA-IM synthesis rate, since experiments performed in primary hepatocytes demonstrated comparable results among the k-in lines. In contrast, secretion of human apolipoproteins into the medium was reduced in both apoA-IM and apoA-I/A-IM hepatic cells compared to apoA-I hepatocytes, reflecting the apolipoprotein levels detected in mouse plasma. These data suggest that an impaired apoA-IM hepatic secretion contributes to the reduction of apoA-IM plasma levels observed in human carriers. Although speculative, reduced apoA-IM secretion may be related to a different intracellular processing (i.e. dimerization) and/or transport of the mutant apolipoprotein.

The possible kinetic basis for the decreased plasma apoA-I and A-IM levels in apoA-IM carriers was previously examined by radiolabeling normal and mutant apoA-I and injecting them into normal and apoA-IM subjects (31). This study has shown that the hypoalphalipoproteinemia in apoA-IM carriers is apparently caused by the rapid catabolism of both apoA-I and apoA-IM, with a normal production rate of the normal and mutant forms of apoA-I. ApoA-IM also appeared to be catabolized more rapidly as a monomer than as a dimer. The clinical study was thus not wholly consistent with our observation that apoA-IM secretion is impaired. Further, a more recent study by Perez-Mendez et al. (32), evaluating the turnover

kinetics of apoA-I- and apoA-IM-specific subclasses using stable isotope techniques, also corroborated these earlier findings, by indicating that hypercatabolism of apoA-I and apoA-IM accounted for a major reduction in apoA-I and HDL in human carriers, while total apoA-I production rate appeared not to be altered. However, detailed examination of the data also indicates that production rates for apoA-IM monomers and apoA-IM dimers are considerably lower than for normal apoA-I. These observations are consistent with our finding that the hepatic secretion of apoA-IM is impaired. In conclusion, we suggest that both factors, i.e. reduced secretion of apoA-IM and rapid catabolism of normal and mutant apoA-I, are major contributors to the hypoalphalipoproteinemia found in human apoA-IM carriers.

## REFERENCES

1. Murray, C. J. L., and Lopez, A. D. (1997) *Lancet* **349**, 1269-1276
2. Stampfer, M. J., Sacks, F. M., Salvini, S., Willett W. C., and Hennekens, C. H. (1991) *N. Engl. J. Med.* **325**, 373-381
3. Genest, J. Jr., McNamara, J. R., Ordovas, J. M., Jenner, J. L., Silberman, S. R., Anderson, K. M., Wilson, P. W., Salem, D. N., and Schaefer, E. J. (1992) *J. Am. Coll. Cardiol.* **19**, 792-802
4. Colyvas, N., Rapp, J. H., Phillips, N. R., Stoney, R., Perez, S., Kane, J. P., and Havel, R. J. (1992) *Circulation* **85**, 1286-1292
5. Grundy, S.M. (1998) *Am. J. Cardiol.* **81**, 18B-25B

6. Robins, S. J., Collins, D., Wittes, J. T., Papademetriou, V., Deedwania, P. C., Schaefer, E. J., McNamara, J. R., Kashyap, M. L., Hershman, J. M., Wexler, L. F., and Rubins, H. B. (2001) *JAMA* **285**, 1585-1591
7. Rubins, H. B., Davenport, J., Babikian, V., Brass, L. M., Collins, D., Wexler, L., Wagner, S., Papademetriou, V., Rutan, G., and Robins, S. J. (2001) *Circulation* **103**, 2828-2833
8. Badimon, J. J., Fuster, V., and Badimon L. (1992) *Circulation* **86**, III86-III94
9. Miyazaki, A., Sakuma, S., Morikawa, W., Takiue, T., Miake, F., Terano, T., Sakai, M., Hakamata, H., Sakamoto, Y., Naito, M., Ruan, Y., Takahashi, K., Ohta, T., and Horiuchi, S. (1995) *Arterioscler. Thromb. Vasc. Biol.* **15**, 1882-1888
10. Chiesa, G., Monteggia, E., Marchesi, M., Lorenzon, P., Laucello, M., Lorusso, V., Di Mario, C., Karvouni, E., Newton, R. S., Bisgaier, C. L., Franceschini, G., and Sirtori, C. R. (2002) *Circ Res.* **90**, 974-980
- 11. Fielding, C. J., and Fielding P. E. (1995) *J. Lipid Res.* **36**, 211-228**
- 12. Stein, O., and Stein, Y. (1999) *Atherosclerosis.* **144**, 285-301**
13. Cockerill, G. W., Huehns, T. Y., Weerasinghe, A., Stocker, C., Lerch, P. G., Miller, N. E., and Haskard, D. O. (2001) *Circulation* **103**, 108-11
14. Sorenson, R. C., Bisgaier, C. L., Aviram, M., Hsu, C., Billecke, S., and La Du, B. N. (1999) *Arterioscler. Thromb. Vasc. Biol.* **19**, 2214-2225
15. Talmud, P., Ye S., Humphries, S. (1982) *Genet. Epidemiol.* **45**, 161-179
16. Reymer, P. W., Gagne, E., Groenemeyer, B. E., Zhang, H., Forsyth, I., Jansen, H., Seidell, J. C., Kromhout, D., Lie, K. E., and Kastelein, J. A. (1995) *Nature Genetics.* **10**, 28-34
17. Kuivenhoven J. A., de Knijff, P., Boer, J. M. A., Smalheer, H. A., Botma, G. J.,

- Seidell, J. C., Kastelein, J. J., and Pritchard, P. H. (1997) *Arterioscler. Thromb. Vasc. Biol.* **17**, 560-568
18. Breckenridge, W. C., Little, J. A., Alaupovic, P., Wang, C. S., Kuksis, A., Kakis, G., Lindgren, F., and Gardiner, G. (1982) *Atherosclerosis* **45**, 161-179
  19. Lopez, D., Sandhoff, T. W., and McLean, M. P. (1999) *Endocrinology* **140**, 3034-3044
  20. Kuivenhoven, J. A., Pritchard, H., Hill, J., Frohlich, J., Assmann, G., and Kastelein, J. (1997) *J. Lipid Res.* **38**, 191-205
  21. Brooks-Wilson, A., Marcil, M., Clee, S. M., Zhang, L. H., Roomp, K., van Dam, M., Yu, L., Brewer, C., Collins, J. A., Molhuizen, H. O., Loubser, O., Ouelette, B. F., Fichter, K., Ashbourne-Excoffon, K. J., Sensen, C. W., Scherer, S., Mott, S., Denis, M., Martindale, D., Frohlich, J., Morgan, K., Koop, B., Pimstone, S., Kastelein, J. J., Genest, J. Jr., and Hayden, M. R. (1999) *Nat Genet.* **22**, 336-34
  22. Assmann, G., von Eckardstein, A., and Funke, H. (1993) *Circulation* **87**, 28-34
  23. Franceschini, G. (1996) *Eur J Clin Invest* **26**, 733-746
  24. Rader, D. J., Ikewaki, K., Duverger, N., Feuerstein, I., Zech, L., Connor, W., Brewer, H. B. Jr. (1993) *Lancet* **342**, 1455-1458
  25. Gualandri, V., Franceschini, G., Sirtori, C. R., Gianfranceschi, G., Orsini, G. B., Cerrone, A., and Menotti, A. (1985) *Am. J. Human Genet.* **37**, 1083-1097
  26. Sirtori, C. R., Calabresi, L., Franceschini, G., Baldassarre, D., Amato, M., Johansson, J., Salvetti, M., Monteduro, C., Zulli, R., Muiesan, M. L., and Agabiti-Rosei, E. (2001) *Circulation* **103**, 1949-1954
  27. Weisgraber, K. H., Bersot, T. P., Mahley, R. W., Franceschini, G., and Sirtori, C.

- R. (1980) *J Clin Invest* **66**, 901-907
28. Rader, D. J., Gregg, R. E., Meng, M. S., Schaefer, J. R., Zech, L. A., Benson, M. D., and Brewer, H. B. Jr. (1992) *J Lipid Res.* **33**, 755-763
29. Tilly-Kiesi, M., Lichtenstein, A. H., Ordovas, J. M., Dolnikowski, G., Malmstrom, R., Taskinen, M. R., and Schaefer E. J. (1997) *Arterioscler Thromb Vasc Biol* **17**, 873-880
30. McManus, D. C., Scott, B. R., Franklin, V., Sparks, D. L., and Marcel, Y. L. (2001) *J Biol Chem.* **276**, 21292-21302
31. Roma, P., Gregg, R. E., Meng, M. S., Ronan, R., Zech, L. A., Franceschini, G., Sirtori, C. R., and Brewer, H. B. Jr. (1993) *J. Clin. Invest.* **91**, 1445-1452
32. Perez-Mendez, O., Bruckert, E., Franceschini, G., Duhal, N., Lacroix, B., Bonte, J.P., Sirtori, C., Fruchart, J.C., Turpin G., and Luc, G. (2000) *Atherosclerosis.* **148**, 317-325
33. Bielicki, J.K., Forte, T.M., McCall, M.R., Stoltzfus L.J., Chiesa G., Sirtori C.R., Franceschini G., and Rubin E.M. (1997) *J Lipid Res.* **38**, 2314-2321
34. Chiesa, G., Stoltzfus, L. J., Michelagnoli, S., Bielicki, J. K., Santi, M. Forte, T. M., Sirtori, C. R., Franceschini, G., and Rubin, E. M. (1998) *Atherosclerosis* **136**, 139-146
35. Williamson, R., Lee, D., Hagaman, J., and Maeda, N. (1992) *Proc. Natl. Acad. Sci. USA* **89**, 7134-7138
36. Walsh, A., Ito, Y., and Breslow, J. L. (1989) *J. Biol. Chem.* **264**, 6488-6494
37. Paszty, C., Mohandas, N., Stevens, M. E., Loring, J. F., Liebhaber, S. A., Brion, C. M., and Rubin, E. M. (1995) *Nature Genet.* **11**, 33-39
38. Koller, B. H., Kim, H. S., Latour, A. M., Brigman, K., Boucher R, C. Jr., Scambler,

- P., Wainwright, B., Smithies, O. (1991) *Proc. Natl. Acad. Sci. USA* **88**, 10730-10734
39. Allain, C. C., Poon, L. S., Chan, C. S., Richmond, W., and Fu, P. C. (1974) *Clin. Chem.* **20**, 470-475
40. Schultz, J. R., Gong, E. L., McCall, M. R., Nichols, A. V., Clift, S. M., and Rubin, E. M. (1992) *J. Biol. Chem.* **267**, 21630-21636
41. Havel, R. J., Eder, H. A., and Bragdon, J. H. (1955) *J. Clin Invest.* **34**, 1345-19
42. Nichols, A. V., Krauss, R. M., and Musliner, T. A. (1986) *Methods in Enzymology* **128**, 417-431
- 43. Gianazza, E. (2002) *The Protein Protocol Handbook*, Wlaker, J.M.; ed, pp. 169-180, Humana Press, Totow**
- 44. Gianazza, E., Giacon, P., Sahlin, B., and Righetti, P. G. (1985) *Electrophoresis* **6**, 53-56**
45. Laemmli, U. K. (1970) *Nature.* **227**, 680-685
46. Görg, A., Postel, W., Weser, J., Günther, S., Strahel, S. R., Hanash, S.M., and Somerlit, L. (1987) *Electrophoresis* **8**, 122-124
47. Chomczynski, P., and Sacchi, N. (1987) *Anal. Biochem.* **162**, 156-159
48. Hayek, T., Ito, Y., Azrolan, N., Verdery, R. B., Aalto-Setälä, K., Walsh, A., and Breslow, J. L. (1993) *J. Clin Invest.* **91**, 1665-1671
49. Azrolan, N., Odaka, H., Breslow, J. L., and Fisher, E. A. (1995) *J. Biol. Chem.* **270**, 19833-19838
50. Bradford, M. M. (1976) *Anal Biochem.* **72**, 248-254
51. Ghiselli, G., Rohde, M. F., Tanenbaum, S., Krishnan, S., and Gotto, A. M Jr. (1985) *J Biol Chem.* **260**, 15662-15668

52. Capecchi, M. R. (1989) *Science* **244**, 1288-1292
53. Franceschini, G., Baio, M., Calabresi, L., Sirtori, C. R., and Cheung, M. C. (1990) *Biochim Biophys Acta* **1043**,1-6
54. Calabresi, L., Franceschini, G., Burkybile, A., and Jonas, A. (1997) *Biochem Biophys Res Commun* **232**, 345-349
55. Franceschini, G., Calabresi, L., Tosi, C., Sirtori, C. R., Fragiaco, C., Nosedà, G., Gong, E., Blanche, P., and Nichols, A. V. (1987) *Arteriosclerosis*. **7**, 426-435
56. Marzal-Casacuberta, A., Blanco-Vaca, F., Ishida, B. Y., Julve-Gil, J., Shen, J., Calvet-Marquez, S., Gonzalez-Sastre, F., and Chan, L. (1996) *J Biol Chem* **271**, 6720-6728

## FIGURE LEGENDS

Figure 1. **Strategy for targeted replacement of the mouse apoA-I gene with the human apoA-I or apoA-IM gene.** A, endogenous mouse apoA-I and apoC-III loci, each with four exons (black boxes). B, the targeting construct containing the 5' and 3' arms of mouse homology (black lines and boxes) interrupted by the human apoA-I or apoA-IM gene (hatched boxes 2', 3', and 4'); the neomycin-resistant (neo) and Thymidine Kinase (T-k) genes are for positive-negative selection of the targeted cells, and pPN2T is the plasmid vector. C, the resulting chimeric gene after homologous cross-over now coding human apoA-I or apoA-IM. Size of diagnostic fragments is indicated. Probe 1, and 2 are a 800 bp SacI–XbaI fragment, and a 350



bp XbaI–SphI fragment, respectively. Restriction sites are as follows: H, HindIII; B, BamHI; E, EcoRI; S, SacI; N, NotI; K, KpnI.

**Figure 2. Southern blot analysis.** A, Southern blot of genomic DNA from six ES cell colonies digested with HindIII and hybridized to Probe 1 (see Fig. 1). Parental cell DNA is in lanes 1 and 6; the 12-Kb band indicates the presence of the unmodified apoA-I allele. Lanes 2-3 and lanes 4-5 contain DNA from human apoA-I and apoA-IM colonies, respectively, that have been correctly targeted; a 9.1-Kb band is present in addition to the 12-Kb band. B, Southern blot analysis of tail DNA digested with HindIII and hybridized to Probe 2 (see Fig. 1) to identify F2 mice carrying the targeted allele. A 3.8-Kb band indicates the presence of the human apoA-I allele. Shown are two controls (lanes 1 and 6), two heterozygous (lanes 2 and 5), and two homozygous (lanes 3-4) k-in mice. Lanes 2-3 and lanes 4-5 contain tail DNA from A-I and A-IM k-in mice, respectively.

**Figure 3. Close-up views of 2-dimensional electrophoretic maps of mouse sera pools obtained from control, A-IM k-in, A-I/A-IM k-in, and A-I k-in mice under non-reducing (upper panel, - $\beta$  ME) and reducing (lower panel, + $\beta$  ME) conditions.**

Proteins were first resolved according to charge on a non-linear pH 4-10 IPG, then fractionated according to size by SDS-PAGE, and stained with Coomassie R-250. The circle indicates the spot corresponding to the dimeric form of human apoA-IM.

**Figure 4. Nondenaturing GGE of mouse lipoproteins.** Total lipoproteins ( $d < 1.215$  g/ml) were loaded onto a nondenaturing 4-30% polyacrylamide gradient gel, and proteins were stained with Coomassie R-250. Computer-assisted scanning densitometry of the gel was used to determine electrophoretic pattern and particle size as described under “Experimental procedures”. HDL particle size distribution of

A-IM k-in (solid line), A-I/A-IM k-in (dashed line), and A-I k-in (dotted line) mice.

**Figure 5. Quantitative Northern blot analysis of apoA-I gene expression in liver.** RNA was prepared from livers of A-IM, A-I/A-IM, and A-I k-in mice, Northern blotted, and hybridized with a human apoA-I probe that spans the majority of human exon 4. The bar graph in the upper portion of the figure shows the amount of apoA-I mRNA corrected for the amount of constitutively expressed  $\beta$ -actin mRNA. In the lower panel, representative blots from each of the three mouse genotypes are shown. Bar graphs represent mean  $\pm$  SD.

Figure 6. In vitro analysis of apoA-I or apoA-IM secretion from primary hepatocytes. Hepatocytes were prepared from A-IM k-in, A-I/A-IM k-in, and A-I k-in mice and the presence of the human apolipoproteins in the medium (normalized to cell protein content) was determined at 30, 60, 90 and 120 min after addition of [ $^3$ H]-leucine. Triangles indicate apoA-IM, open squares indicate apoA-I/A-IM and diamonds indicate apoA-I secretion. The data are representative of three separate experiments; each point is the mean  $\pm$  SD of triplicate measurement.

Table I. Plasma lipid profiles and human apolipoprotein concentration in k-in and control mice

Mice	n	TC (mg/dl)	FC (mg/dl)	HDL-C (mg/dl)	TG (mg/dl)	apoA-I or apoA-IM (mg/dl)
A-IM k-in	9	52.89±5.87 <sup>ab</sup>	21.21±2.32 <sup>cd</sup>	28.08±5.00 <sup>e</sup>	33.08±24.12	100.68±19.43 <sup>c</sup>
A-I/A-IM k-in	8	78.07±5.46	19.29±1.45	56.68±1.96	29.41±14.34	107.78±30.18 <sup>c</sup>
A-I k-in	8	132.04±34.58	38.26±9.09	75.46±14.85	31.78±21.75	213.70±41.76
Controls	5	106.80±7.76	29.37±2.30	57.29±3.00	57.61±20.30	—

<sup>a</sup> p<0.001 vs A-I k-in, and control mice.

<sup>b</sup> p<0.05 vs A-I/A-IM k-in mice

<sup>c</sup> p<0.001 vs A-I k-in mice

<sup>d</sup> p<0.05 vs control mice

<sup>e</sup> p<0.001 vs A-I k-in, A-I/A-IM k-in, and control mice

Results are expressed as means±SD; TC, total cholesterol; FC, free cholesterol; TG, triglyceride.

Figure 1

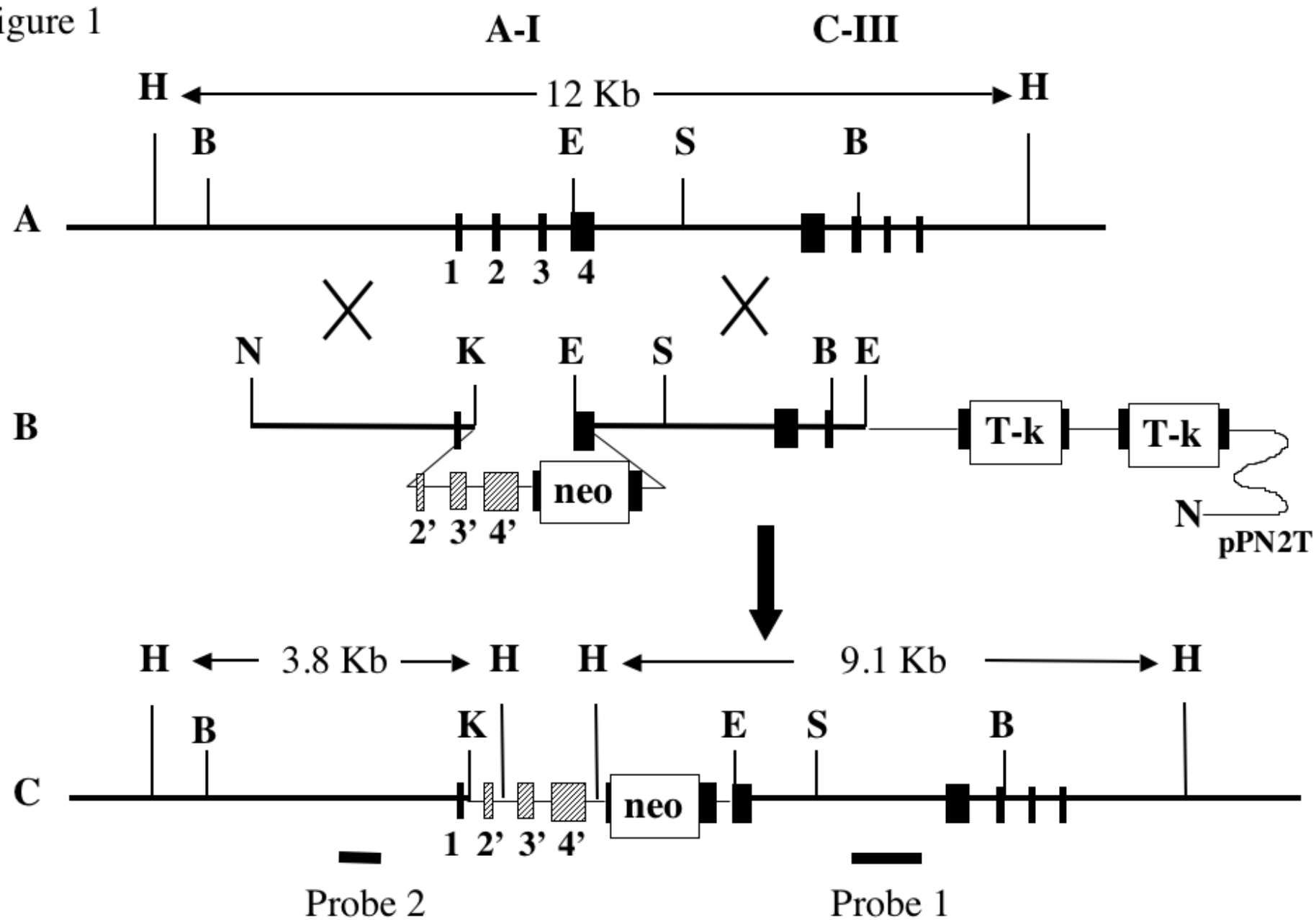


Figure 2

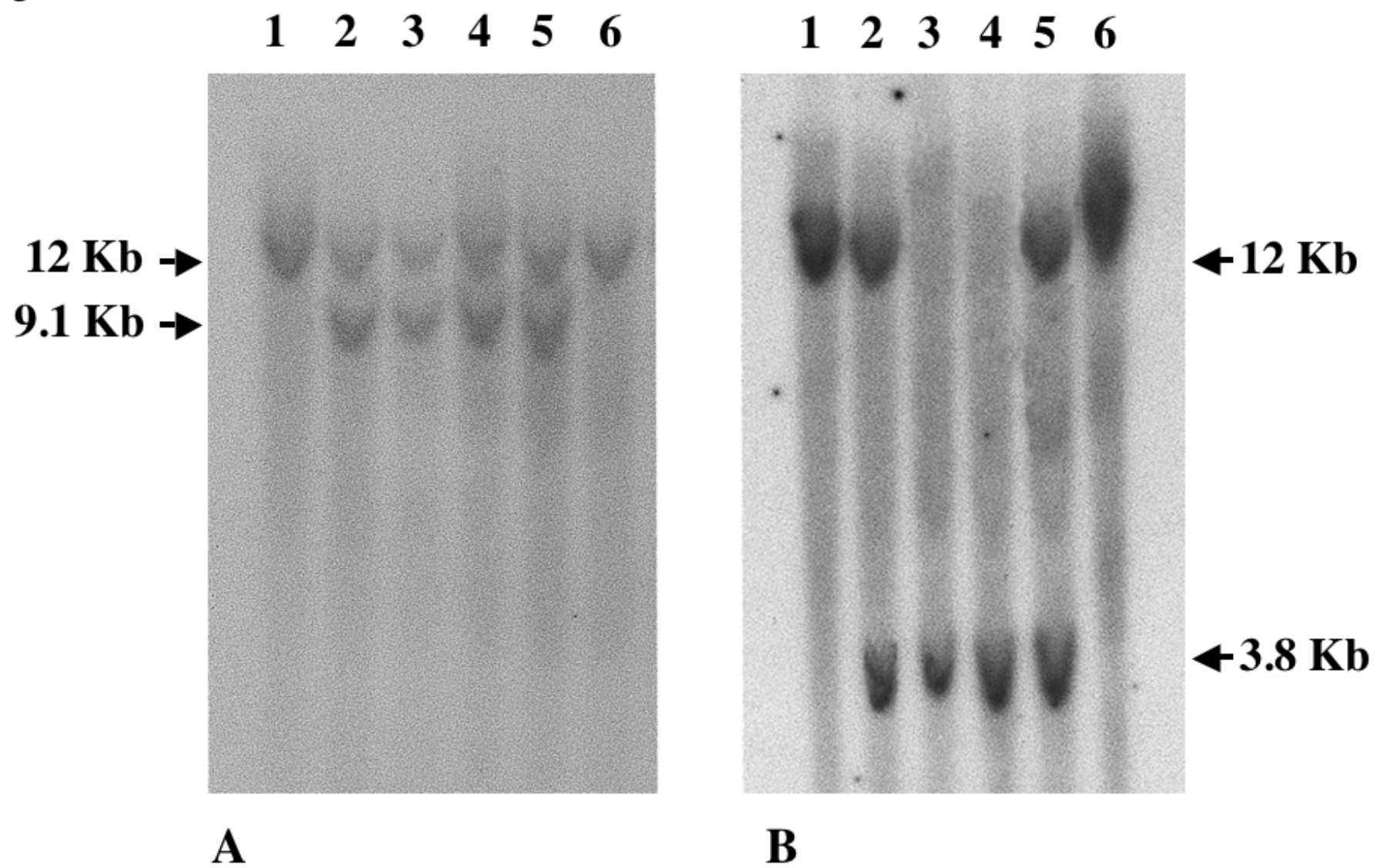


Figure 3

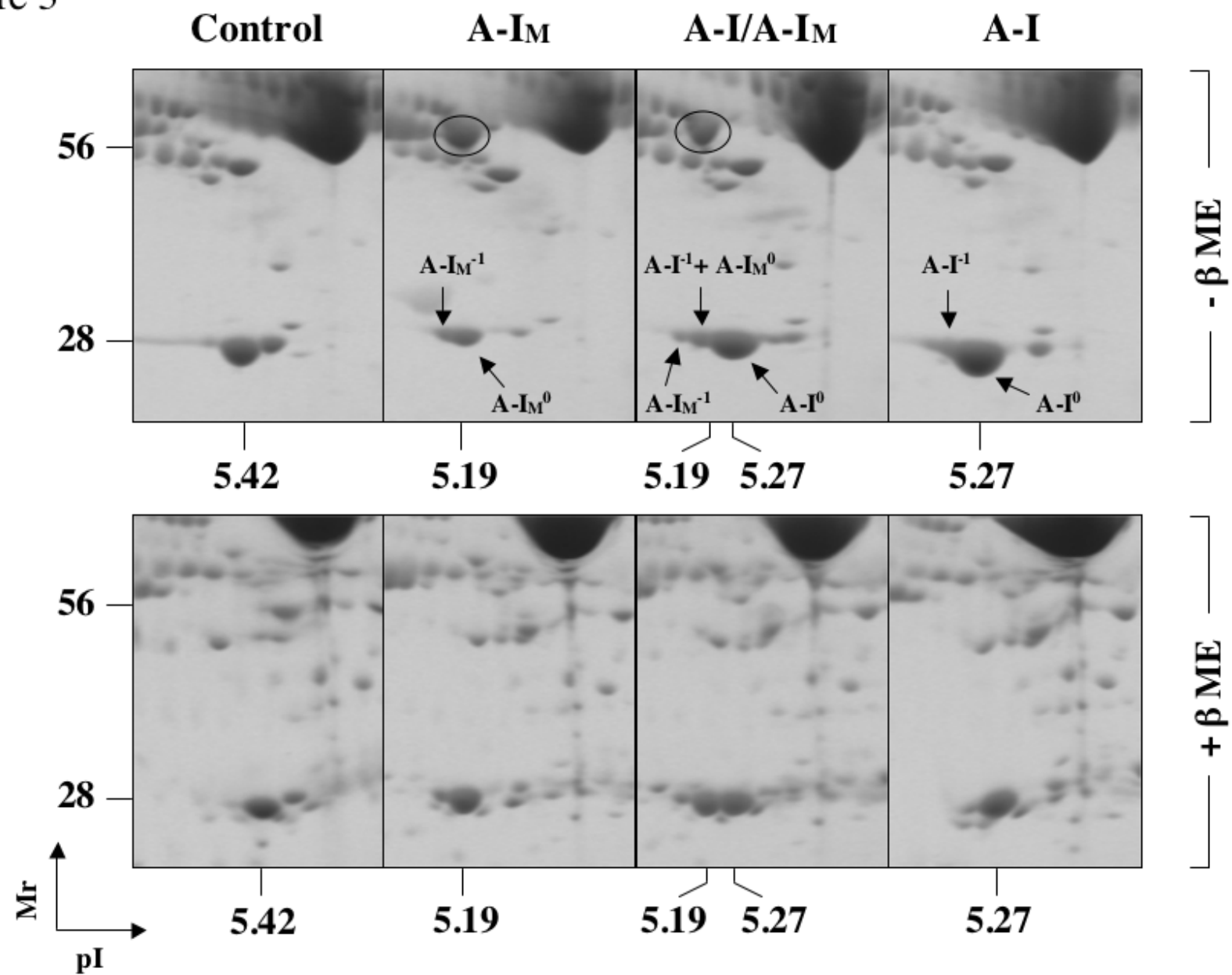


Figure 4

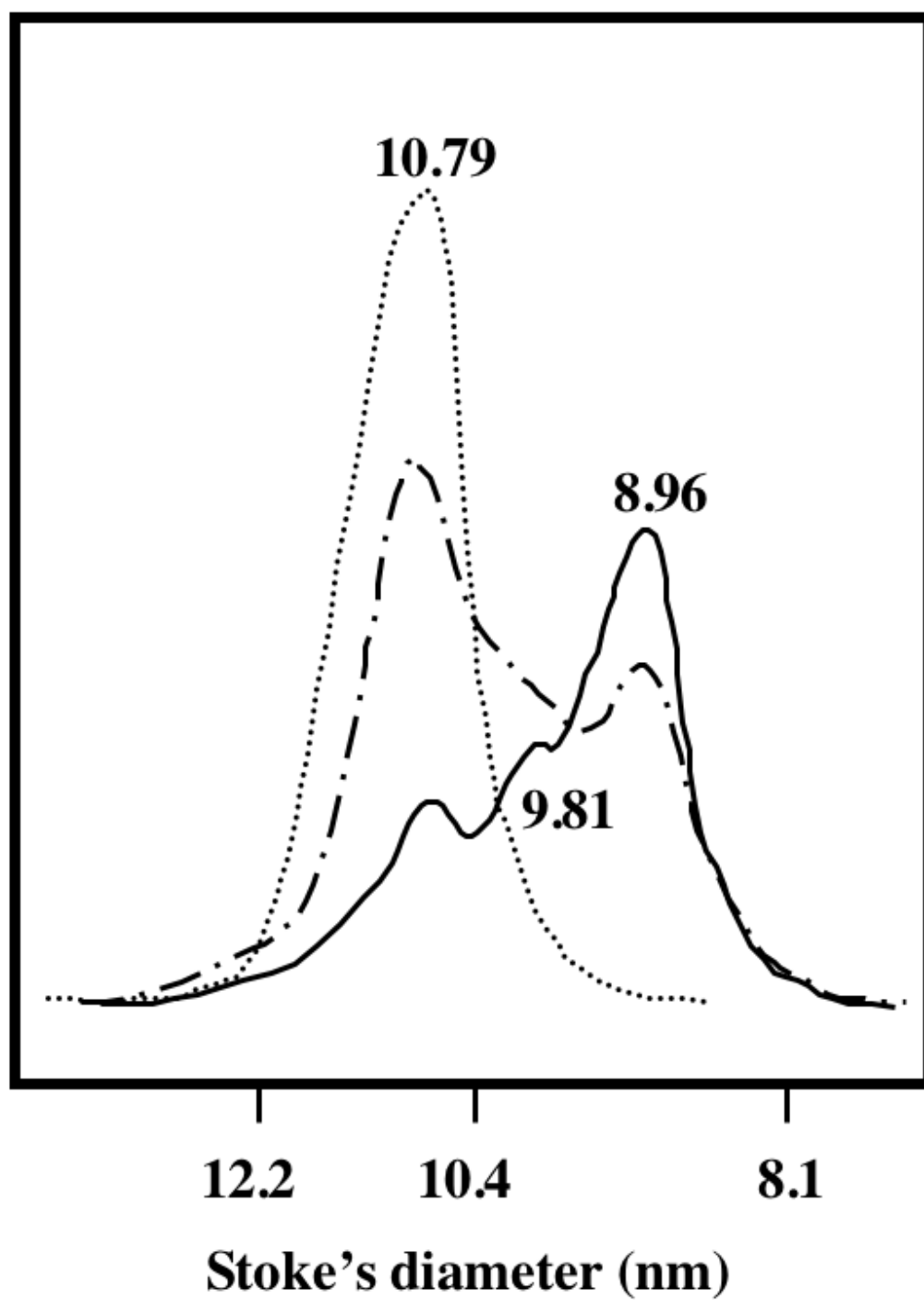


Figure 5

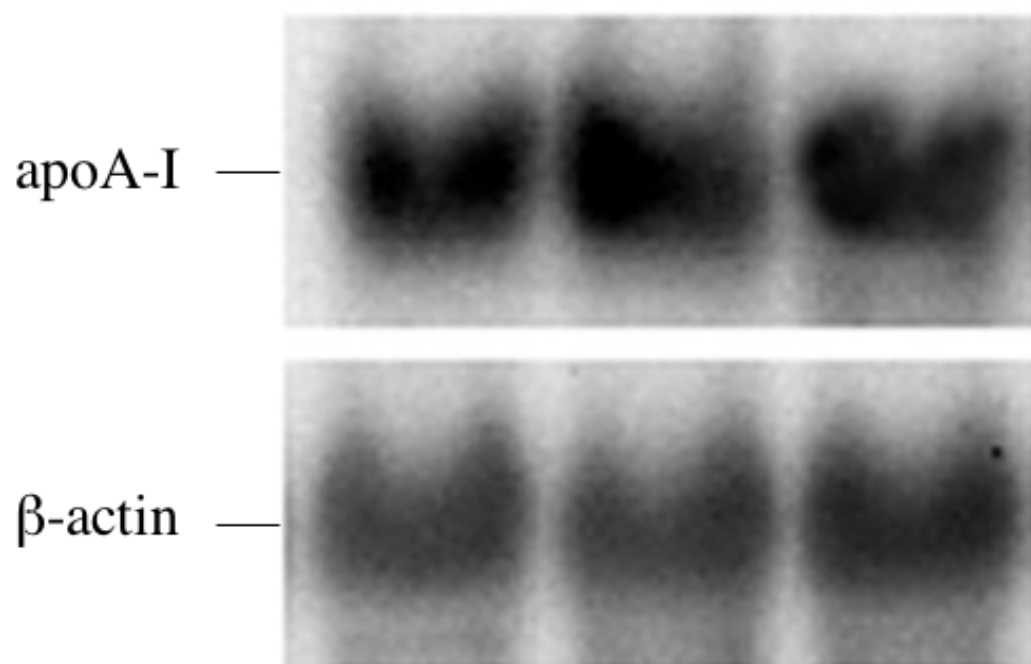
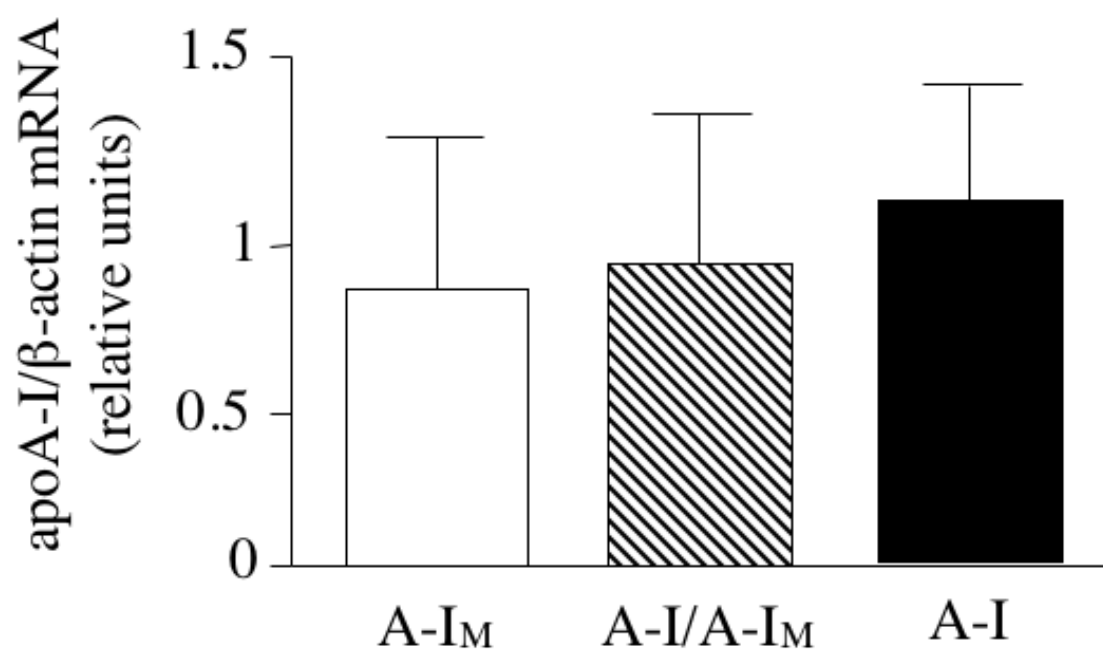




Figure 6

